

An upper limit for slow earthquakes zone: Self-oscillatory behavior through the Hopf bifurcation mechanism from a model of spring-block under lubricated surfaces

Valentina Castellanos-Rodríguez¹, Eric Campos-Cantón², Rafael Barboza-Gudiño³, and Ricardo Femat⁴

^{1,3}Instituto de Geología, Universidad Autónoma de San Luis Potosí, México.

^{1,2,4}Instituto Potosino de Investigación Científica y Tecnológica A.C., San Luis Potosí, México.

² Mathematics Department, University of Houston, Houston, Texas 77204-3008, USA.

Correspondence to: Castellanos-Rodríguez Valentina (valentina@cimat.mx)

Abstract. The complex oscillatory behavior of a springblock model is analyzed via the Hopf bifurcation mechanism. The mathematical spring-block model includes Dieterich-Ruina's friction law and Stribeck's effect. The existence of self-sustained oscillations in the transition zone-where slow earthquakes are generated within the frictionally unstable region -is determined. An upper limit for this region is proposed as a function of seismic parameters and frictional coefficients which are concerned with presence of fluids in the system. The importance of the characteristic length scale L , the implications of fluids, and the effects of external perturbations in the complex dynamic oscillatory behavior as well as in the stationary solution, are take into consideration.

1 Introduction

In the last decade, the study of slow earthquakes (tremors, low and very low frequencies events, and slow slip events) has taken a great relevance because of its possible relationship with the occurrence of large earthquakes. The stress redistribution of slow earthquakes, and the strain in the lowest limit of the seismogenic layer caused by them, could be helpful for a better understanding of the nucleation process of ordinary earthquakes (Ide *et al.*, 2007; Wech and Creager, 2007; Beroza and Ide, 2009; Peng and Gomberg, 2010; Rivet *et al.*, 2011; Ikari *et al.*, 2013; Jolivet *et al.*, 2013; Abe and Kato, 2014; Audet and Bürgmann, 2011; Bürgmann, 2014; Wallace *et al.*, 2016). Although the most slow earthquakes have been detected in subduction zones, there are reports of these in other types of faults (Vergnolle *et al.*, 2010; Thomas *et al.*, 2016; Wallace *et al.*, 2016).

Observations suggest that this occurs between the seismogenic zone and the frictionally stable zone (Fig. 1) surrounding the critical value of ordinary earthquakes nucleation; *i.e.*, on parts of faults where the behavior is transitional between frictional properties on the rocks and slow, steady deformation (Scholz, 1998; Dragert *et al.*, 2001; Beroza and Ide, 2009; Abe and Kato, 2014; Watkins *et al.*, 2015), but some investigation reveal that have been observed in shallow region (Davis *et al.*, 2011; Nishimura, 2014; Saffer and Wallace, 2015; Valée *et al.*, 2015; Yamashita *et al.*, 2015; Wallace *et al.*, 2016). Figure 1 shows two stability regions and transition zones: at shallow depth, and on the base of seismogenic layer (Scholz, 1998) which is the focus of the study presented in this paper.

Scholz (1998) determined that at the border of the stability transition there is a region in which self-sustained oscillatory (SSO) motion occurs into the conditionally stable region, below the critical point, and slow earthquakes are nucleated. These oscillations are observed in presence or absence of external forces such as vibrations from neighbor faults but eventually tend to stabilize.

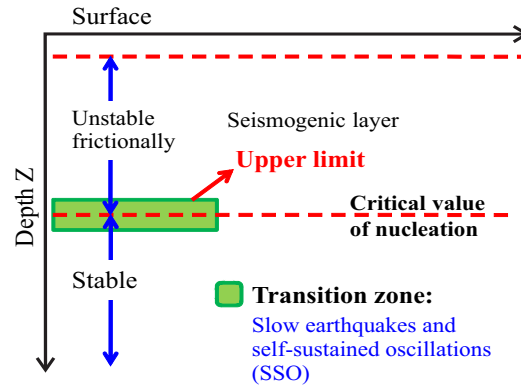


Figure 1. Transition zone related to slow earthquakes nucleation. The first dashed red line indicates the lowest limit of the shallow frictionally stable region. The second one shows the deeper limit of the seismogenic layer (upper limit of the deeper frictionally stable region). Self-oscillatory behavior is observed in the second transition.

5 Slow earthquakes occur in a variety of stick-slip (Ide *et al.*, 2007). Watkins *et al.* (2015) say that observational studies have provided information for their characterization: variability in duration, recurrence and propagation velocity, but the mechanism of slow earthquakes is still unclear. Experimental data show that the physical and mechanical parameters that control changes in slow slip events are the rates of convergence, frictional parameters and effective normal stress, under rate and state dependent constitutive properties of Dieterich-Ruina friction law (Dieterich, 1979; Ruina, 1983; Watkins *et al.*, 2015; Marone *et al.*, 2015; Scuderi *et al.*, 2016).

The Dieterich-Ruina friction law has been successfully used to reproduce the stick slip behavior in the models of earthquakes dynamics and slow earthquakes. Spring-block models have reproduced these events when coupled with rate and state dependent friction laws, and contrary, models which have been used laws velocity-weakening friction and constant friction have not been successful (Abe and Kato, 2014). Beroza and Ide (2009) infer that simple friction laws by themselves do not provide an explanation for the complex behavior of slow earthquakes. Some investigations have suggested that fluids play an important role in this mechanism (Brown *et al.*, 2005; Ide *et al.*, 2007; Wallace *et al.*, 2016). Some researches support this idea, conclusions from revised literature establish that failures are lubricated on the shear area regardless of the composition of the rocks and the frictional weakening mechanism involved (Faulkner *et al.*, 2010; Di Toro *et al.*, 2011).

An important issue of the rate and state dependent friction law is that it is totally macroscopic, *i. e.*, it describes the frictional properties of the system rather than microscopic mechanism which is responsible for the dissipation (Ruina, 1983; Carlson and Batista, 1996; Batista and Carlson, 1998). Experimental research on the role of fluids in the ordinary earthquakes mechanism

has captured specific features associated with the molecular layer lubrication on the border between two surfaces in contact, with different frictional properties when considering lubricants in volume and dry interfaces (Gee *et al.*, 1990; Yoshizawa and Israelachvili, 1993; Reiter *et al.*, 1994; Carlson and Batista, 1996; Batista and Carlson, 1998; Amendola and Dragoni, 2013). The initiation slip in the microscopic scale is associated with a shear melting transition in the lubricant layer (Carlson and Batista, 1996) so that microscopic scales contribute to better understanding of friction mechanism.

A path to study slow earthquakes is through spring-block model for ordinary earthquakes, because both the slow and ordinary earthquakes are related by the critical value of nucleation. Some spring-block models display complex oscillatory behavior associated with the transition zone (Gu *et al.*, 1984; Abe and Kato, 2013, 2014). Gu *et al.* (1984) and Abe and Kato (2013), used a spring-block model where complex oscillatory behavior was found near to a critical value of the earthquakes nucleation. This behavior is presented as changing when there is a variation in any parameter related to the critical value.

Batista and Carlson (1998) in a spring-block model introduced an alternative friction law, where the state variable is interpreted in terms of the shear melting of the lubricant (molecular layer of lubricant) between solid surfaces in contact. They considered that by incorporating the microscopic mechanism it could determine other behavior and found that the transition from steady sliding to stick slip is typically discontinuous and sometimes hysteretic. This transition is associated with a sub-critical Hopf bifurcation (set of seismic parameters for the critical point of nucleation). Gu *et al.* (1984), Abe and Kato (2013), and Batista and Carlson (1998) observed a sudden and discontinuous onset in the amplitude of oscillations at the bifurcation point. At surrounding of transition, complex oscillatory behavior was observed in these cases.

In terms of dynamical systems based on spring-block model, the presence of oscillations and self-oscillations can be explained by Hopf bifurcation mechanism (Kengne *et al.*, 2014; Xin-YouMeng and Hai-Feng Huo, 2014; Wang *et al.*, 2014). Some nonlinear dynamical systems show *SSO* motion (Strogatz, 1994), one of them is relative to the earthquake physics mechanism (Scholz, 1998). The *SSO* behavior would be explained in the context of the complex system of faults, such that the modeling of movement in a single failure would be affected by external forces (Chelidze *et al.*, 2005). These forces can be generated due to vibrations or stress transferred from neighboring faults, that make the system going from a limit cycle to another, leaving different paths of recurrence (Chelidze *et al.*, 2005; Dragoni and Santini, 2010; Dragoni and Piombo, 2011).

In this paper the main objective is to propose an upper limit for the *SSO* region in the frictionally unstable zone (Fig. 1). The upper limit is a function of mathematical and numerical relations in terms of seismic and frictional parameters. This limit describes the complexity of the oscillatory movement in the nearest region to the critical point of nucleation. Another objective is determine which is the role of the fluids in this region. The oscillatory behavior of the system is studied through analysis of the Madariaga's spring-block model (Erickson *et al.*, 2008) complemented by the Stribeck's effect (Alvarez-Ramírez *et al.*, 1995; Andersson *et al.*, 2007). The Stribeck's effect shows the transition from dry interfaces or lubricated at the border until separated by a layer of lubricant as a shear melting. This effect takes into account the microscopic mechanism between the contacting surfaces during displacement. The Dieterich-Ruina-Stribeck oscillator (Fig. 2) depicts the behavior of the kinetic mechanism between tectonic blocks in the earth's crust undergoing stick-slip effects from friction. The oscillator is coupled to a driven plate by the rheological properties of rocks, and to a static plate by frictional properties. The slider is on the rough and

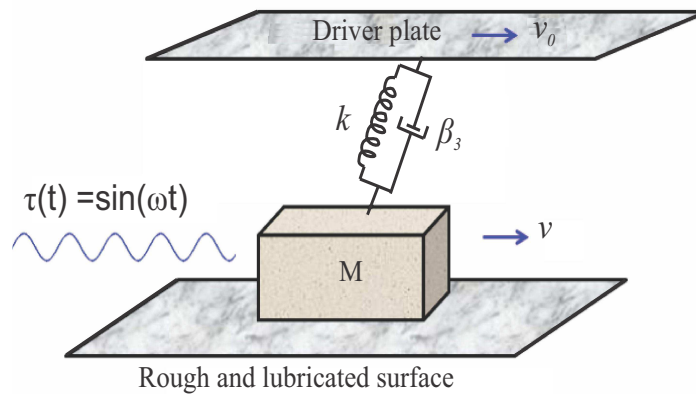


Figure 2. Dieterich-Ruina-Stribeck one degree of freedom oscillator. v_0 is a reference velocity, v is the block velocity, k is the constant of deformation, β_3 is the dynamical viscosity coefficient. $\tau(t)$ is an external and perturbing force with angular frequency ω .

lubricated surface. The relative displacement, rate of displacement and acceleration are given by $u = y - v_0 t$, $\dot{u} = v - v_0$, and $\ddot{u} = \dot{v}$ respectively where y is the block displacement and $v = \dot{y}$. An external periodic perturbation $\tau(t)$ is introduced in order to show that this system exhibits *SSO* behavior between the critical point of nucleation and the region limited by the proposed upper limit. In Section 2 the model is proposed, the linearized system, stationary solution and criterion for frictional stability are analyzed; in Section 3 the oscillatory behavior is described, the upper limit of *SSO* region is proposed and numerical simulations are provided. Finally, in Section 4 a brief discussion of the outcomes and conclusions are presented.

2 Nonlinear Dynamical System

2.1 The model

The faults are lubricated in the shear area (Faulkner *et al.*, 2010; Di Toro *et al.*, 2011) as the most sliding contacts. A model based in a slider block (Fig. 2) is essentially a mechanic representation, and the frictional components are velocity dependent. Andersson *et al.* (2007) explain the Stribeck's effect as follows. The friction force varies with the sliding speed depending on the extent to which the interacting contact surfaces are running under boundary, mixed (fluid in the union between asperities), or full film lubrication (a layer of fluid as a shear melting). Even dry contacts show some behavior similar to that in lubricated contacts in that they have a higher static friction than dynamic or sliding friction. In lubricated sliding contacts, the friction decreases with increasing sliding speed until a mixed or full film situation is obtained, after which the friction in the contact can be constant, increasing or decreasing somewhat with increasing sliding speed due to viscous and thermal effects. This

transition is the named Stribeck's effect (Jacobson, 2003; Andersson *et al.*, 2007) and has been formulated as :

$$F_s(v) = \beta_1 \text{sign}(v - v_0) + \beta_2 e^{-\mu(v)} \text{sign}(v - v_0) + \beta_3 v, \quad (1)$$

where β_1 is the Coulomb friction; $\beta_2 = F_{max} - \beta_1$ (with F_{max} as the upper limit of static force); β_3 represents the dynamical viscosity coefficient of the fluid; and μ denotes a slip constant or decay parameter for the mixed lubrication.

- 5 On the other hand, the well known phenomenological friction law of Dieterich-Ruina is introduced in rocks mechanics to capture experimental observations of steady state and transient friction that depends on the displacement history effects (state variable θ) and velocity (Dieterich, 1979; Ruina, 1983; Dieterich and Kilgore, 1994), one of its formulations is given by two equations (Ruina, 1983):

$$F_{dr}(v, \theta) = \theta + A \ln(v/v_0), \quad \dot{\theta} = -(v/L)[\theta + B \ln(v/v_0)]. \quad (2)$$

- 10 First equation represents the frictional stress under stable state ($\dot{\theta} = 0$), and the second one corresponds to evolution of state variable θ that evolves with time, slip, and normal stress history (Dieterich and Kilgore, 1994). L is a characteristic sliding distance over which θ evolves (required distance to renew the contact population). A and B are material properties, we assume $B > A > 0$ for frictional instability.

- Now it is possible to derive from Eqs. (1) and (2) an alternative friction law taking into account the macroscopic and
 15 microscopic mechanism (frictional properties and dissipation). The equation of motion derived from Eqs. (1) and (2) gives a first order differential equation system, a similar expression is given by Erickson *et al.* (2008), but we complemented their system by the term of Stribeck's effect:

$$\begin{aligned} \dot{\theta} &= -(v/L)[\theta + B \ln(v/v_0)], \\ \dot{u} &= v - v_0, \\ \dot{v} &= -(1/M)[ku + F_{dr}(v, \theta)] - (1/M)F_0(v) + \tau(t), \end{aligned} \quad (3)$$

where the Stribeck's effect from Eq. (1) is given now by

$$20 \quad F_0(v) = \beta_1 + \beta_2 e^{-\mu(v)} + \beta_3 v. \quad (4)$$

- Note that the slider block velocity is relative to velocity of driver plate. From the second equation of the system (3), we infer that the block will oscillate with respect to the position of the plate. This equation tells us whether the oscillator is to the right or to the left with respect to the driver plate. Although the direction of the displacement of the system is always forward; if $v - v_0 > 0$, *i.e.*, if $v > v_0$, eventually the oscillator will be more advanced than the plate. On the other hand, if $v - v_0 < 0$, *i.e.*,
 25 $v < v_0$ eventually the oscillator will be to the left of the plate. One of the objectives when introducing the function $\text{sign}(v - v_0)$ in the Eq. (1) is indicate this effect; assigning value 1 for the first case, -1 for the second case, and zero otherwise. We eliminate the sign function because this effect is already considered in the second equation of the system (3).

Defining new variables $\hat{\theta}$, \hat{v} , \hat{u} and \hat{t} (Erickson *et al.*, 2008): $\theta/A = \hat{\theta}$, $v/v_0 = \hat{v}$, $u/L = \hat{u}$, $t(v_0/L) = \hat{t}$, the dimensionless system is given by the following equations

$$\begin{aligned}\dot{\hat{\theta}} &= -\hat{v}[\hat{\theta} + (1 + \varepsilon)\ln(\hat{v})], \\ \dot{\hat{u}} &= \hat{v} - 1, \\ \dot{\hat{v}} &= -\gamma^2[\hat{u} + (1/\xi)(\hat{\theta} + \ln(\hat{v}))] - \alpha F_0(\hat{v}) + \hat{\tau}(\hat{t}),\end{aligned}\tag{5}$$

where $\alpha = \{\alpha_1, \alpha_2, \alpha_3\}$; $\alpha_{1,2} = \frac{L\beta_2}{v_0^2 M}$, $\alpha_3 = \frac{L\beta_3}{v_0 M}$. The external force is $\hat{\tau}(\hat{t}) = \hat{c}\sin(\hat{\omega}\hat{t})$, where $\hat{c} = \frac{L}{v_0^2}$ and $\hat{\omega} = \frac{L\omega}{v_0}$. The frictional parameters α are associated with frictional coefficients from the Stribeck's effect and

$$\alpha F_0(\hat{v}) = \alpha_1 + \alpha_2 e^{-\hat{\mu}\hat{v}} + \alpha_3 \hat{v}, \quad \hat{\mu} = v_0 \mu.\tag{6}$$

$x = (\hat{\theta}, \hat{u}, \hat{v})$ is the dimensionless state variable, $\hat{\theta}$ stands for the measurement of contact with asperities from the Dieterich-Ruina friction law; \hat{u} is the dimensionless relative displacement between the block and the upper plate and $\hat{v} > 0$ is the dimensionless velocity of the block. The function $f(x)$ on the right-hand side of Eq. (5) defines a mapping $f: \mathbb{R}^3 \rightarrow \mathbb{R}^3$. This mapping defines a vector field on \mathbb{R}^3 . Thus, the system given by Eq. (5) induces in phase space \mathbb{R}^3 the flow (φ^t) , $t \in \mathbb{R}$ such that each forward trajectory of the initial point $x_0 = x(t=0)$ is the set $\{x(t) = \varphi^t(x_0) : t \geq 0\}$.

Parameters $\Pi = (\varepsilon, \xi, \gamma)$ are given as follows: $\varepsilon = (B - A)/A$; $\xi = kL/A$ and $\gamma = \sqrt{(k/M)}(L/v_0)$, associated with stress drop during displacement, deformation and the oscillation frequency, respectively. The Equation (5) is referred to the system of Dieterich-Ruina-Stribeck (DR-S) where $\tau(\hat{t}) = [0, 0, \hat{\tau}(\hat{t})]^T$ is the periodical and deterministic external force $\hat{\tau}(t) = \hat{c}\sin(\hat{\omega}t)$, here $\hat{\omega}$ is the angular frequency. We named unperturbed system when $\hat{\tau}(t) = 0$ and perturbed system otherwise. We will denote $(\hat{\theta}, \hat{u}, \hat{v}) := (\theta, u, v)$, $\hat{\tau}(\hat{t}) := \tau(t)$, $\hat{\omega} := \omega$, $\hat{c} := c$, and $\hat{\mu} := \mu$.

2.2 Stationary solution at equilibrium point

The stationary solution $x = x^*$ of the system (5) with $\tau(t) = 0$ is given by

$$x^* = (\theta^*, u^*, v^*) = (0, \eta, 1), \quad u^* = \eta = (\alpha_1 + \alpha_2 e^{-\mu} + \alpha_3)/\gamma^2, \quad \gamma > 0,\tag{7}$$

where η corresponds to the relative position of the single slider block. At x^* the plate and the block have the same velocity and the measure of the asperities contact is zero. Note that θ^* and v^* do not depend on Π but u^* depends on frequency oscillation γ (consequently on kL) and frictional constants of Stribeck's effect, both are associated with the energy dissipation.

In the spring-block model, the logarithmic term in the Dieterich-Ruina's friction law has introduced greater difficulty to solve the problem. Due to the nonlinear term, analytic integration has not been possible, and even numerical solutions present challenges because of the logarithmic term (Erickson *et al.*, 2008). The linearized system analysis is very useful to describe some features of the nonlinear system about steady state solution (Gu *et al.*, 1984; Shkoller and Minster, 1997; Erickson *et al.*, 2008). The local and asymptotic stability of x^* is analyzed with the indirect method of Lyapunov that consists in the analysis of the eigenvalues of the Jacobian matrix from the linearized system of Eq. (5) around the stationary solution (Khalil, 1996). Let

x^* be locally asymptotically stable, *i. e.*, every solution of the system $\varphi^t(x_0) = (\theta(t), u(t), v(t))$, starting near of the stationary solution, it remains at the surrounding of x^* all the time, and eventually the solution converges to x^* (convergence to frictional stability). Let us denote the Jacobian matrix as $D_f(x^*) = (\partial f_i(x)/\partial x_j)|_{x^*}$, for $i, j = 1, 2, 3$, where $f(x) = (f_1, f_2, f_3)$ is the vector field given by the right-hand side of (5) with $\tau(t) = 0$; $(x_1, x_2, x_3) = (\theta, u, v)$; and let λ_i be the eigenvalues of $D_f(x^*)$:

$$5 \quad D_f(x^*) = \begin{pmatrix} -1 & 0 & -(1+\varepsilon) \\ 0 & 0 & 1 \\ -\gamma^2/\xi & -\gamma^2 & -\gamma^2/\xi - \phi \end{pmatrix} \quad (8)$$

where $\phi = \alpha_2 \mu e^{-\mu} - \alpha_3$. The characteristic polynomial of (8) is given by:

$$P(\lambda) = a_0 \lambda^3 + a_1 \lambda^2 + a_2 \lambda + a_3, \quad (9)$$

whose coefficients are in terms of seismic parameters Π , and frictional coefficients α and μ .

$$a_0 = 1; \quad a_1 = 1 + \gamma^2/\xi + \phi; \quad a_2 = \gamma^2(1 - \varepsilon/\xi) + \phi; \quad a_3 = \gamma^2. \quad (10)$$

10 The dynamical system of earthquakes is a naturally dissipative phenomena due to this feature the dissipativity condition of the stationary solution is required. Thus locally the system is dissipative at x^* if $a_1 = -\text{Trace}D_f(x^*) = \sum_{i=1}^3 \lambda_i < 0$ that is true under the condition:

$$\frac{Mv_0}{L} + \frac{A}{v_0} + \beta_2 \mu e^{-\mu v_0} < \beta_3; \quad (11)$$

Equation (11) comes directly from $a_1 < 0$ and the values of γ , ε , ξ , and ϕ . The Equation (11) is the necessary condition for the system to be sub-damped, and oscillations can be observed; moreover due to $a_3 = -\det D_f(x^*) < 0$, x^* is hyperbolic. Through the analysis of the eigenvalues of $D_f(x^*)$ we will explain what implies a hyperbolic equilibrium point related to oscillatory behavior.

3 Oscillatory Behavior

The earthquakes dynamics is a nonlinear oscillatory phenomenon (Gu *et al.*, 1984; De Sousa Vieira, 1995; Levin, 1996; Chelidze *et al.*, 2005; Maloney and Robbins, 2007; Erickson *et al.*, 2008; Dragoni and Santini, 2010; Castellanos-Rodríguez and Femat, 2013; Amendola and Dragoni, 2013; Abe and Kato, 2014); where the nonlinear complex behavior is attributable to the friction forces. The analysis of the oscillatory behavior is explored in this section. We use the full nonlinear term in the numerical simulation in Section 3.2 and 3.3.

3.1 Analysis of Eigenvalues

25 The equilibrium point x^* is locally asymptotically stable if the real part of all the eigenvalues is negative, *i.e.* $Re(\lambda_i) < 0$, and it is unstable if at least one eigenvalue of $D_f(x^*)$ is positive, *i.e.* $Re(\lambda_i) \geq 0$. We are interested in the type of hyperbolic

stationary solution $x^* = (0, \eta, 1)$: it has a stable manifold; *i.e.*, $Re\{\lambda_i\} < 0$, $Im\{\lambda_i\} = 0$, and a unstable manifold that generates oscillations in a plane, *i.e.*, $Re\{\lambda_k\} > 0$, $Im\{\lambda_k\} \neq 0$ (Campos-Cantón *et al.*, 2010). A sufficient condition for local and asymptotic stability comes from the Routh-Hurwitz criterion, *i. e.*, the sufficient conditions to ensure that Jacobian matrix (8) has three eigenvalues with negative real part is that the coefficients of the characteristic polynomial holds the inequalities:

$$5 \quad a_0, a_1, a_2, a_3 > 0 \quad a_1 a_2 - a_0 a_3 > 0. \quad (12)$$

Note that the first inequality holds: $a_0, a_3 > 0$, and $a_1 > 0$ because $\phi < 1$ and $\Pi > 0$; if $sign(a_2) > 0$ we deduce

$$\varepsilon < \xi\psi; \quad \psi = 1 + \phi/\gamma^2; \quad (13)$$

as a necessary condition for stability but it is not sufficient. The sufficient condition for stability comes from the second inequality of (12) and $a_2 > 0$ as follow

$$10 \quad \varepsilon < \xi \left[1 - \frac{1}{1 + \gamma^2/\xi + \phi} + \frac{\phi}{\gamma^2} \right]. \quad (14)$$

For the region with the sufficient condition (14), all eigenvalues of the Jacobian matrix (8) have negative real part and the

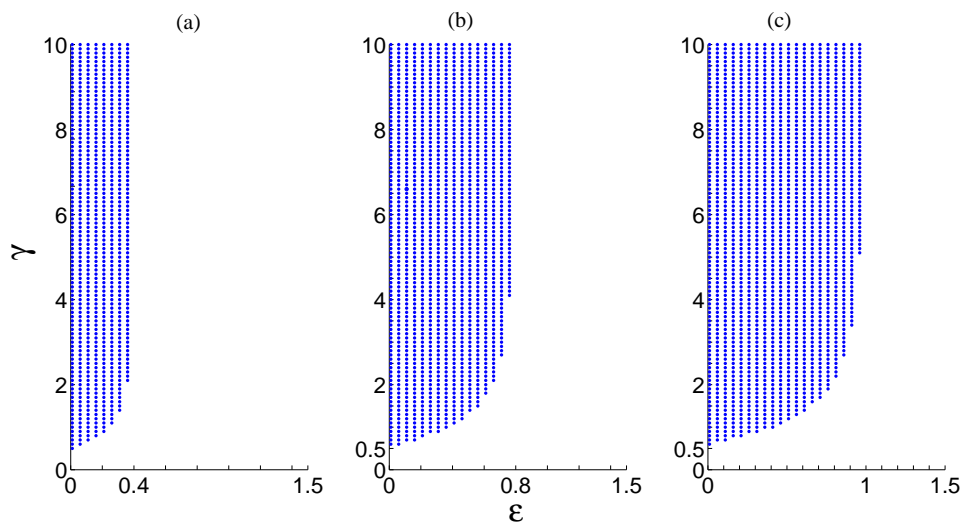


Figure 3. Stability region for homogeneous system ($\tau(t) = 0$), as a function of $(\varepsilon, \xi, \gamma)$ for fixed values of ξ . (a) $\xi = 0.4$, (b) $\xi = 0.8$, and (c) $\xi = 1$. The necessary and sufficient conditions are satisfied.

equilibrium point $x^* = (0, \eta, 1)$ is a sink (Perko *et al.*, 2001).

The relationship between the parameters Π associated with the necessary condition (13) and sufficient condition (14) are described in Figures 3 (a), (b) and (c), for fixed $\xi = 0.4, 0.8, 1$, respectively. By means of numerical simulation the stability was

15 computed and found for values of $\gamma > 0.5$.

In order to determine how many eigenvalues of $D_f(x^*)$ are real or complex conjugate, Descartes' rule of signs to analyze the roots of the characteristic polynomial is used. Under the condition (11), signs of coefficients (10) are

$$(+, +, \text{sign}(a_2), +). \quad (15)$$

If $\text{sign}(a_2) > 0$ there are two possibilities: all eigenvalues are negative real, i. e., $\text{Re}\{\lambda_i\} < 0, \text{Im}\{\lambda_i\} = 0$ or one eigenvalue is negative real and the other two are complex conjugates; the last statement corresponds to the oscillatory behavior.

On the other hand, if $\text{sign}(a_2) < 0$, there are possibly two positive real eigenvalues, i.e., $\text{Re}\{\lambda_k\} > 0, \text{Im}\{\lambda_k\} = 0$ and one negative real; for this case there are no complex conjugate eigenvalue, hence non-oscillatory behavior is observed. For all cases there is one negative real eigenvalue, the other two could be complex conjugates or positive real. Figure 4 shows the locus of the real part of two eigenvalues corresponding to the oscillatory and the non-oscillatory behavior, it describes the relationship between parameters Π . The graph for the negative real eigenvalue was omitted because we focused on complex eigenvalues. The oscillatory behavior is located before the branching, after which the system ceases to oscillate. The locus of the eigenvalues

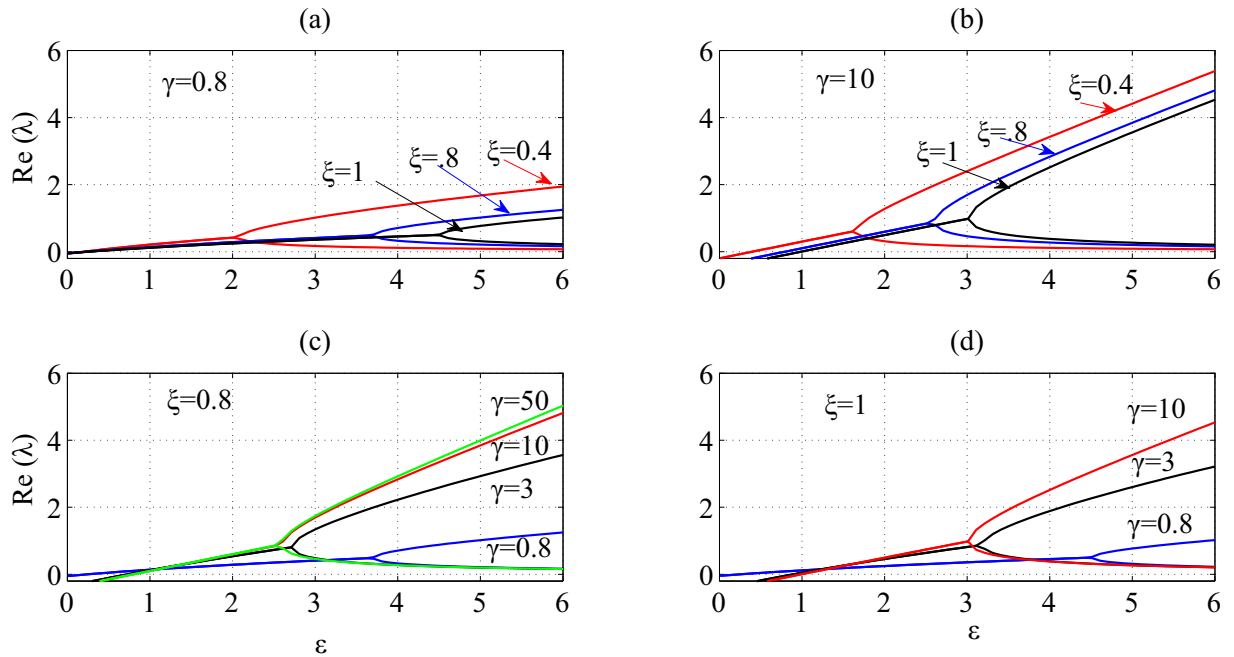


Figure 4. Locus of eigenvalues for different values of ξ and γ . The Figure shows the real part of eigenvalues as a function of parameters ε , ξ and γ . For (a) and (b) fixed $\gamma = 0.8, 10$, respectively; (c) and (d) shows eigenvalues for fixed $\xi = 0.8, 1$ respectively.

for different values of $\xi = 0.4, 0.8, 1$ are shown in Figure 4(a), (b) for $\gamma = 0.8$ and $\gamma = 10$, respectively. The range of ε decreases with the increasing of γ and the decreasing of ξ . Figures 4 (c) and (d) describe the same behavior as explained above, and it was observed that for values of $\gamma > 10$ the range of ε for oscillatory behavior is almost equal, although after the branching

15 point with the increasing of γ , one of the eigenvalues increases rapidly, *i. e.*, kL increases, making biggest the system stiffness or L increases; and the other one tends to zero, more quickly.

It was found a set of parameters that satisfies the necessary condition (13) for stability, within an unstable and oscillatory region which is around of the Hopf bifurcation (set of seismic parameters that satisfies the critical value of nucleation; Fig. 1). The region with these features is proposed for the region of self-sustained oscillations (*SSO*) and consequently for the slow earthquakes zone. The *SSO* region is in the unstable region and will be explored in the follow sections.

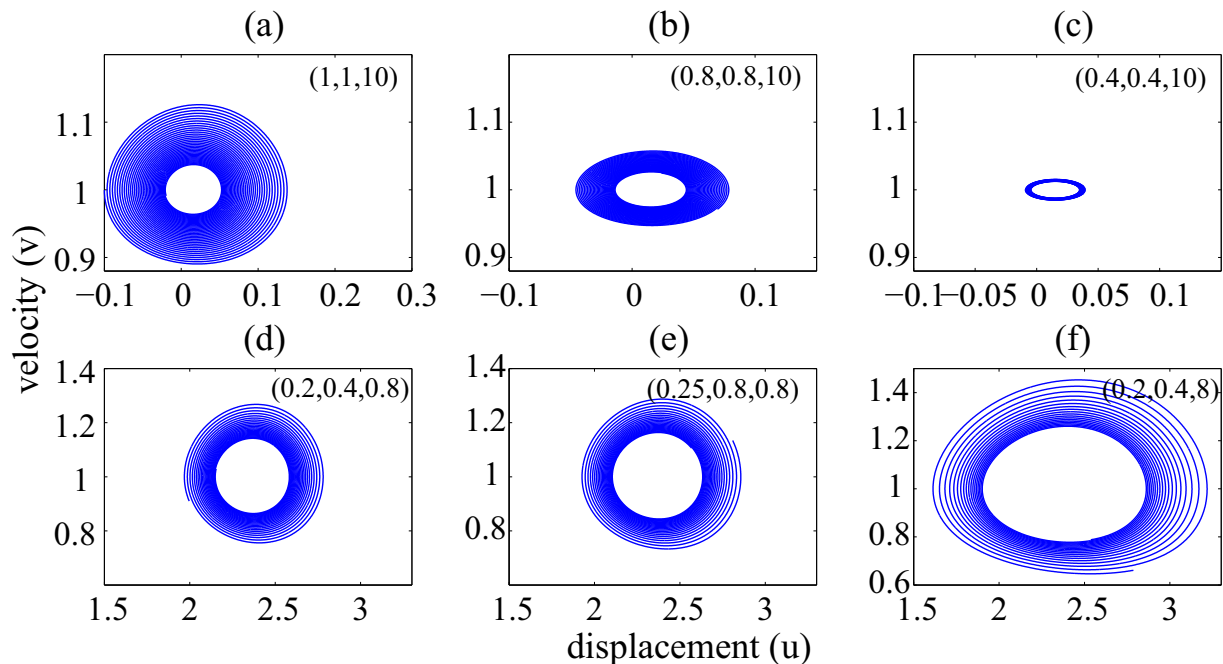


Figure 5. Unperturbed system $\tau(t) = 0$. Projection of attractor onto the plane (u, v) . (a), (b) and (c) have the position of equilibrium point $u^* = \eta$ near zero for $\gamma = 10$, ξ decreases as it is the range of u . (d), (e) and (f), for $\gamma = 0.8$ have both u^* and the range of values for u higher than (a)-(c).

5

3.2 A Hopf Bifurcation, Oscillatory Range (*OR*) and the Self-sustained Oscillations Region (*SSO*)

The presence of oscillations in physical systems can be explained through the mechanism of Hopf bifurcation. When three eigenvalues exist two of them are complex conjugates and the other is a non-zero real, a Hopf bifurcation occurs (Fig. 5) if the real part of the complex eigenvalues cross the imaginary axis. Periodic orbits and limit cycles are either created or destroyed for the nearest values of the Hopf Bifurcation (Guckenheimer and Holmes, 1983). If all neighboring trajectories approach the limit cycle then it can be said that the limit cycle is stable or an attractor. Stable limit cycles are important because they model systems that exhibit *SSO* behavior (Strogatz, 1994), therefore starting at Hopf Bifurcation, the oscillatory behavior around it

will be analyzed.

There are three necessary conditions in order to a Hopf bifurcation may occurs: (i) The existence of an equilibrium point, $f(x^*) = 0$; (ii) the Jacobian matrix $D_f(x^*)$ has a couple of eigenvalues on the imaginary axis, *i. e.*, $Re\{\lambda_{1,2}\} = 0$ and $Im\{\lambda_{1,2}\} \neq 0$; and (iii) the cross velocity of eigenvalues through imaginary axis must be different to zero.

- 5 For any system with three variables the conditions (ii) and (iii) for obtaining a Hopf bifurcation are given in terms of the characteristic polynomial coefficients a_1 , a_2 , and a_3 from Eq. (10) (Baca, 2007). The cross velocity is given by the derivative $r'(\Pi_0) = \frac{d}{d\gamma}(Re\{\lambda(\Pi)\})|_{\gamma=\gamma_0} \neq 0$, where $\Pi_0 = (\varepsilon_0, \xi_0, \gamma_0)$ is a set of fixed values and $\lambda(\Pi)$ is an eigenvalue of $D_f(x^*)$ at Π . The derivative is with respect to the bifurcation parameter, γ (oscillation frequency). The cross velocity is

$$r'(\Pi_0) = \frac{a_3'(\Pi_0) - b^2 a_1'(\Pi_0) + \lambda_0 a_2'(\Pi_0)}{2(\lambda_0^2 + b^2)}, \quad a_1(\Pi_0) = -\lambda_0 \text{ and } a_2(\Pi_0) = b^2. \quad (16)$$

- 10 The polynomial from Eq. (9) has a couple of imaginary roots $\lambda_{1,2}$ if there is a Π such that the following two relations are satisfied

$$a_3 = a_1 a_2, \quad a_2 > 0. \quad (17)$$

If $\Pi = \Pi_0$ satisfies the Eq. (17), then the complex roots of Eq. (9) with real part zero are determined by

$$\lambda_{1,2} = \pm i b_0 \quad b_0 = \sqrt{a_2}, \quad \lambda_3 = -\frac{a_3}{a_2}. \quad (18)$$

- 15 From Eqs. (10) and (18), the eigenvalues of (8) for the Hopf bifurcation are given by

$$\lambda_{1,2}(\Pi_0) = \pm i \sqrt{\gamma_0^2 - \frac{\gamma_0^2 \varepsilon_{HB}}{\xi_0} + \phi}, \quad \lambda_3(\Pi_0) = -\frac{\gamma_0^2}{\gamma_0^2 - \frac{\gamma_0^2 \varepsilon_{HB}}{\xi_0} + \phi}. \quad (19)$$

The Jacobian matrix (8) has two complex conjugate eigenvalues with positive real part for values of ε which depend on the fixed values γ_0 and ξ_0 . These eigenvalues correspond to oscillatory region in the unstable regime, and they are observed from the Hopf bifurcation to the beginning of bifurcation as it is depicted in the Fig. 4, this interval is called the oscillatory range

- 20 *OR*. We want to find the limits of *OR* and the *SSO* in terms of seismic parameters.

From Eqs. (10) and (17) it is determined ε_{HB} , *i. e.*, the ε value for the Hopf bifurcation

$$\varepsilon_{HB} = \xi_0 \left[1 - \frac{1}{1 + \frac{\gamma_0^2}{\xi_0} + \phi} + \frac{\phi}{\gamma_0^2} \right]. \quad (20)$$

ε_{HB} is the lower limit of *OR*. The upper limit is determined by the discriminant of the third order polynomial $a_0 \lambda^3 + a_1 \lambda^2 +$

- 25 $a_2 \lambda + a_3$:

$$D = \left(\frac{3a_2 - a_1^2}{9} \right)^3 + \left(\frac{9a_1 a_2 - 27a_3 - 2a_1^3}{54} \right)^2, \quad (21)$$

If $D > 0$ there are two complex conjugate roots and one is real, if $D = 0$ all are real roots, and at least two are equal; and if $D < 0$ all roots are real and unequal. We are interested in $D = 0$, which implies that the oscillatory behavior finishes (there are not complex roots). From Eqs. (9), (10), and (21)

$$D = \left[\frac{3 \left(\gamma_0^2 - \frac{\gamma_0^2 \varepsilon_{D=0}}{\xi_0} + \phi \right) - \left(1 + \frac{\gamma_0^2}{\xi_0} + \phi \right)^2}{9} \right]^3 + \left[\frac{9 \left(1 + \frac{\gamma_0^2}{\xi_0} + \phi \right) \left(\gamma_0^2 - \frac{\gamma_0^2 \varepsilon_{D=0}}{\xi_0} + \phi \right) - 27\gamma_0^2 - 2 \left(1 + \frac{\gamma_0^2}{\xi_0} + \phi \right)^3}{54} \right]^2 = 0,$$

5 and we can resolve by $\varepsilon_{D=0}$, according to Fig. 4. The *OR* for ε is in the interval

$$OR \in (\varepsilon_{HB}, \varepsilon_{D=0}). \quad (22)$$

In the *OR*, the necessary condition (13) for stability is satisfied by a set of parameters Π around the Hopf bifurcation; the region with these features is proposed for the *SSO*. The proposed interval for *SSO* is

$$SSO \in (\varepsilon_{HB}, \xi_0 \psi_0), \quad \psi_0 = 1 + \frac{\phi}{\gamma_0^2}. \quad (23)$$

Some numerical results are summarized in Table 1. Our interest is for the case that $\varepsilon = (B - A)/A > 0$, or $B - A > 0$; which

γ	ξ	ε_{HB}	$\pm(\lambda_{1,2})_{HB}$	$\varepsilon_{D=0}$	$SSO \in (\varepsilon_{HB}, \xi_0 \psi_0)$	$r'_\varepsilon(\Pi_0)$
0.8	0.4	0.1981	0.5030i	2.081779482130000	(0.1981,0.3562)	0.3042
	0.8	0.2499	0.6083i	3.704570372000000	(0.2499,0.7123)	0.2058
	1.0	0.2534	0.6385i	4.507300000000000	(0.2534,0.8904)	0.1749
10	0.4	0.3981	0.6313i	1.668570861615000	(0.3981,0.3997)	0.4981
	0.8	0.7931	0.8911i	2.601243068598171	(0.7931,0.7994)	0.4963
	1.0	0.9894	0.9954i	3.018387963893687	(0.9894,0.9993)	0.4953

Table 1. Relationship between parameters Π on the oscillatory range for Figures 4 (a) and (b). ε_{HB} : value of the Hopf Bifurcation; $(\pm\lambda_{1,2})_{HB}$: eigenvalues on the imaginary axis; $\varepsilon_{D=0}$: value when the discriminant of the characteristic polynomial is equal to zero, *i. e.* upper limit of *OR*; *SSO* is the interval of self-sustained oscillations, and $r'_\varepsilon(\Pi_0)$ is the cross velocity of eigenvalues.

10

means that the stress drop is negative and consequently an unstable regime is observed; under this assumption, $\xi\psi$ it is a positive amount implying that $\psi > 0$. Equation (13) is a necessary condition for stability, which is maintained within a set of values of parameters where the system is unstable (Table 1).

15 In the DR-S model any small perturbation in the system can change the dynamical behavior. If the DR-S system is subject to perturbations from neighboring faults, the seismic fault enters in a limit cycle, but it does not remain long there due to intervening stress perturbations (Dragoni and Santini, 2010).

3.3 The System Under Forcing Conditions

This section aims to numerically describe the oscillatory behavior within and outside the range proposed for the SSO region (23), under forcing and non-forced conditions. We want to prove numerically that the proposed upper limit determines the changes in oscillatory behavior, below and above this. For more theoretical background into the theory of periodically forced systems near a point of Hopf bifurcation, see Zhang and Golubitsky (2011) and references therein.

- 5 We are interested in the oscillatory behavior when the values of parameters Π are nearest to the Hopf bifurcation. We numerically explored the effects of an external, deterministic and periodic force $\tau(t)$ acting on the system (5), for $\Pi=\{0.25,0.8,0.8\}$, $\alpha=\{1.6,0.2,0.1\}$, and $\mu=3$. Such effects are illustrated by varying the angular frequency ω from $\tau(t) = \sin\omega t$. This numerical analysis is helpful visualizing patterns in the dynamic of the system, especially those related to oscillatory behavior, such as limit cycles and periodic orbits. Figure 6 shows numerical results of typical oscillations projected onto the plane (u, v) and

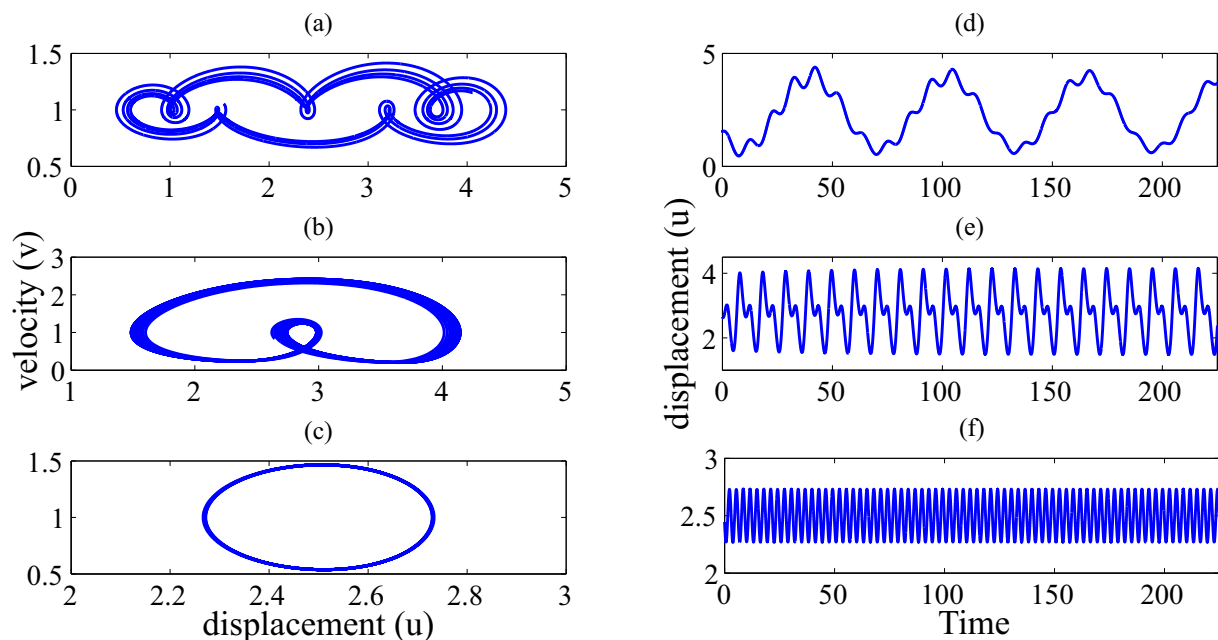


Figure 6. Projection of the attractor onto the plane (u, v) and time series of the perturbed system (5). (a), (b) and (c) show the projection onto the plane for $\omega = 0.1, 1.2, 2$, respectively. (d), (e) and (f) display their respective time series for u .

- 10 time series generated by Eq. (5). The system (5) presents different behaviors when the parameter ω takes values in the interval $[0.1, 2]$. For example when $\omega \in [0.1, 0.8)$, a type of complex behavior for low frequencies is observed (Fig. 6 (a)). Figure 6 (b) shows that for values of $\omega \in [0.8, 1.3)$ periodic orbits of period two are found. For angular frequencies $\omega > 1.3$ the flow of the system converges to a limit cycle as shown in Fig. 6 (c). On the other hand, Figures 6 (d) to (f) describe the time series of u when ω is 0.1, 1.2 and 2, respectively. The motion is periodical, this behavior emphasizes the periodic motion of the DR-S.
- 15 The time series for low frequencies ($\omega < 0.8$) are more complex than the other cases.

3.3.1 Bifurcation Diagram for Unperturbed System

Qualitative changes in the dynamic of the system are better understood through bifurcation analysis such that when a control parameter is varied the bifurcations show the transitions or instabilities of the system. The unperturbed system is considered when $\tau(t) = \sin(\omega t) = 0$, *i. e.*, $\omega = 0$. In order to show that the behavior of the unperturbed system displays SSO, the control parameter $\gamma = \sqrt{(k/M)}(L/v_0)$ is varied, which in turn is related to frequency of oscillation of the slider block and to the characteristic length of displacement L . Numerical results are for fixed $\xi = 0.8$, and the value for $\varepsilon = 0.25$ that holds the necessary condition (13).

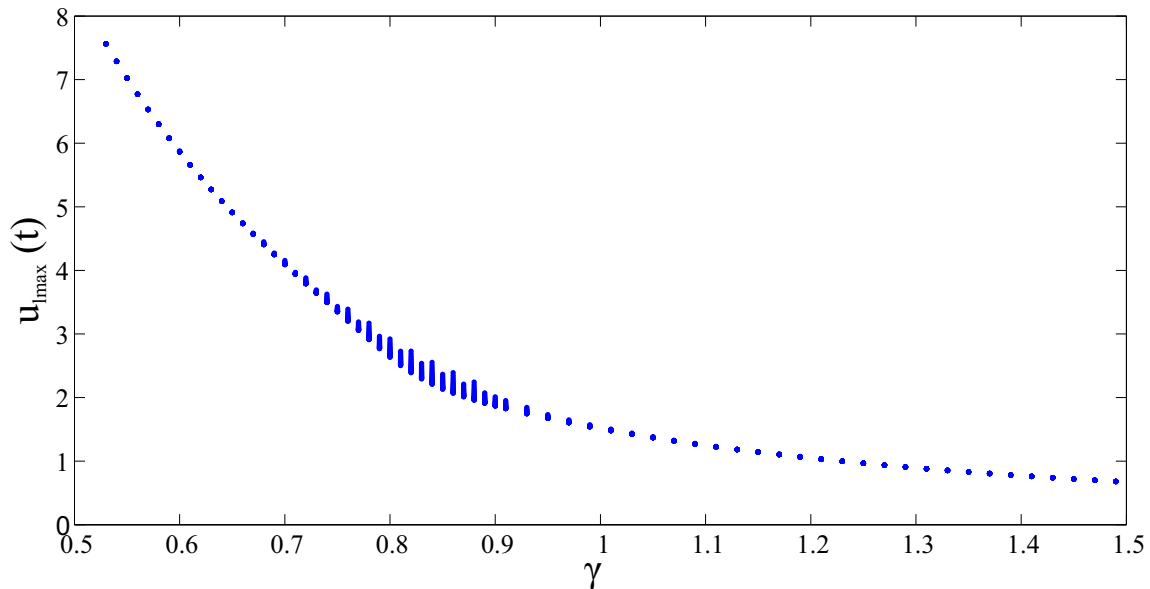


Figure 7. Bifurcation diagram for unperturbed system $\tau(t) = 0$, bifurcation parameter γ versus local maximum of time series $u_{\max}(t)$, $\Pi = \{0.25, 0.8, \gamma\}$.

Under the necessary condition (13), the system without external perturbations oscillates and multi-periodic orbits are created over an approximate range of values $\gamma \in [0.6, 1]$. Eventually, the flow of the system converges to a limit cycle as is depicted in Figures 7 and 8. This oscillatory behavior is observed when Π is nearest to the Hopf bifurcation in absence of external forces.

10 The range of $u_{\max}(t)$ decreases when γ increases.

3.3.2 Bifurcation Diagram for Perturbed System

According to previous outcomes, we considered the forced system $\tau(t) = \sin \omega t$ centered at $\omega = \{0.1, 1.2\}$, for fixed $\xi = 0.8$, and two values of ε . Two values for $\varepsilon = \{0.25, 1\}$ are explored. The first value holds the necessary condition and the second one does not. The bifurcation parameter is γ . We named case one to the analysis of bifurcation with fixed $\varepsilon = 0.25$, and second case
 15 for $\varepsilon = 1$; for both cases $\xi = 0.8$ is fixed. The bifurcation diagram for case one is displayed in Fig. 9, it shows the qualitative

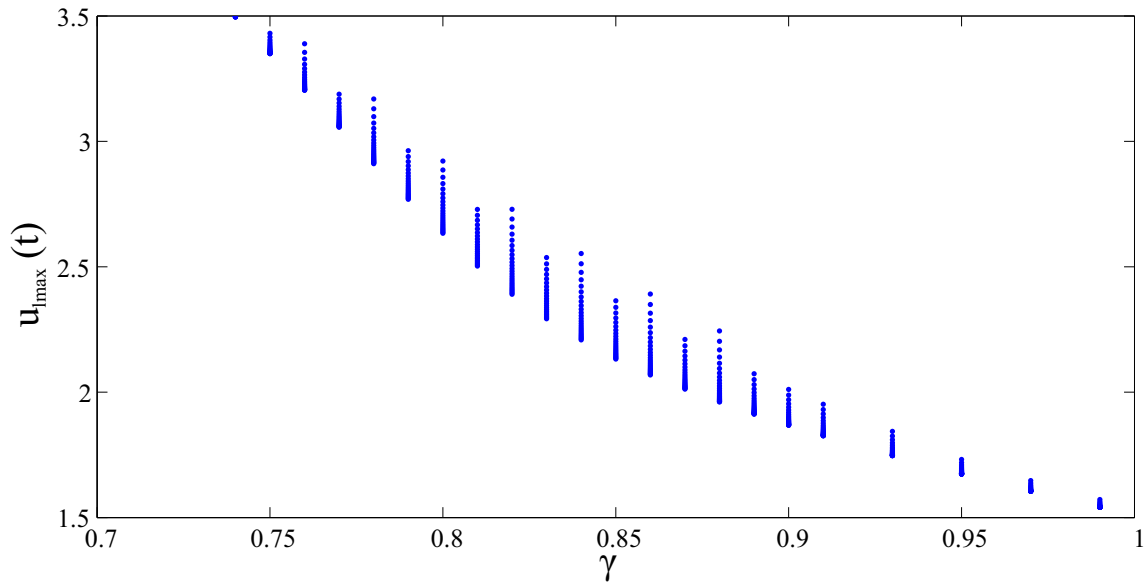


Figure 8. Zoom of Figure 7.

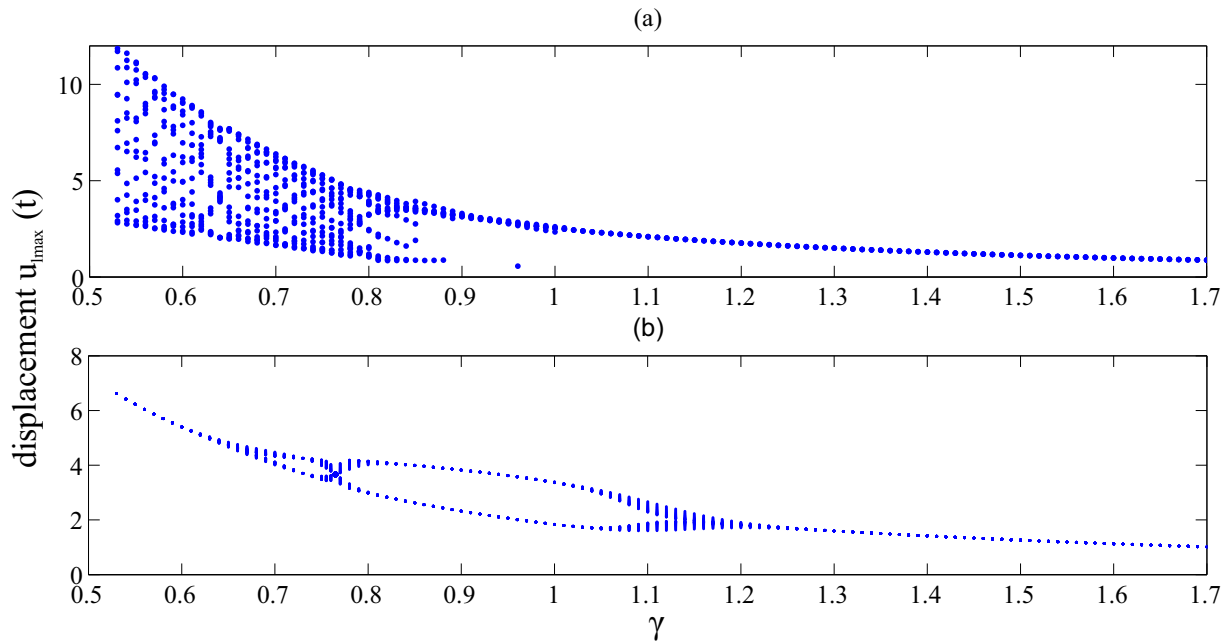


Figure 9. Bifurcation diagram γ versus local maximum from the time series $u_{lmax}(t)$. $\Pi = \{0.25, 0.8, \gamma\}$, $\mu = 3$, $\alpha = \{1.6, 0.2, 0.1\}$, sub-damped system. (a) $\omega = 0.1$, and (b) $\omega = 1.2$.

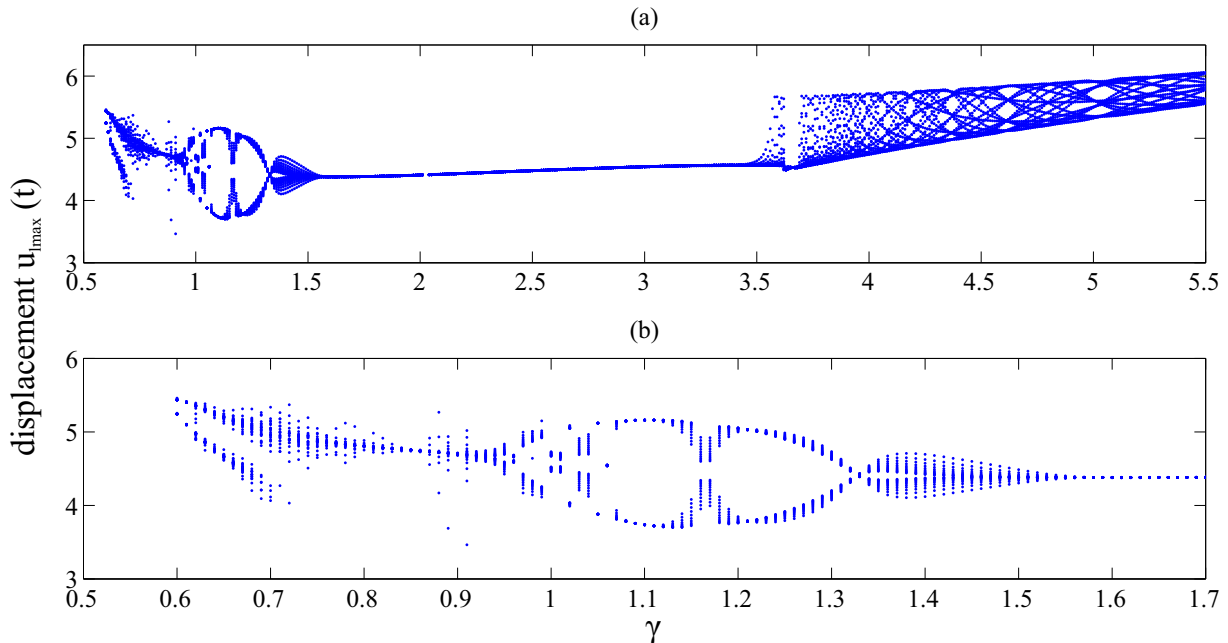


Figure 10. Bifurcation diagram γ versus local maximum from time series $u_{lmax}(t)$, $\omega = 1.2$, $\Pi = \{1, 0.8, \gamma\}$ $\mu = 3$, $\alpha = \{1.6, 0.2, 0.1\}$, sub-damped system. (a) There are three types of behavior: Type I, II and III. (b) Zoom of Type I.

behavior of system relative to the variable of position u and oscillation frequency γ . The Figure 9 displays γ versus its local maximum of time series $u_{lmax}(t)$. Figure 9 (a) for $\omega = 0.1$ shows that the most orbits are weakly attractive until approximate values of $\gamma > 0.9$ when limit cycles are observed.

On the other hand, Fig. 9 (b) for $\omega = 1.2$ shows limit cycles, which are observed approximately when $\gamma \in [0.55, 0.66)$, $\gamma > 1.17$ and $\gamma = .765$; whereas there are two points of bifurcation from orbits of period one to orbits of period two at $\gamma = 0.66$ and $\gamma = 0.765$. The orbits of period two have the form of Fig. 6 (b), and the limit cycles take the form as in Fig. 6 (c). The orbits are strongly attractive, which suggests that they could be stable at least during a short period. According to the necessary condition for stability, the behavior of $u_{lmax}(t)$ relative to γ decreases for both $\omega = 0.1$ and $\omega = 1.2$ because after γ reaching the values 0.9 and 1.17, respectively, the system falls into the limit cycle, in such a way that when γ increases, the range of values for $u_{lmax}(t)$ decrease. The type of behavior displayed in Fig. 9 is expected when $\varepsilon < \xi\psi$.

10 The region of *SSO* could be numerically explained by this analysis; if the system is perturbed slightly by external forces $\tau(t)$, it always returns to the standard cycle.

The bifurcation diagram for case two is displayed in the Fig. 10 (a) for $\omega = 1.2$. The necessary condition (13) fails; and the dynamic of the system shows three types of behavior: behavior Type I (Fig. 10 (b)) is observed approximately at $\gamma \in (0.6, 1.55)$. Type I shows periodic orbits of period one and two that appear to be alternating, bifurcations from orbits of period one to pe-
 15 riod two occur, then the system reaches a limit cycle at $\gamma = 1.55$ but now with Type II behavior for approximate values of

$\gamma \in (1.55, 3.5)$. In the Type II $u_{lmax}(t)$ increases while maintaining the limit cycle until behavior Type III is observed approximately for $\gamma \in (3.5, 5.5)$, which displays periodic orbits with different period. The behavior displayed in Fig. 10 corresponds to unstable and oscillatory region outside of the *SSO*.

3.4 Type of Hopf bifurcation

In terms of the flow in phase space, a supercritical Hopf bifurcation occurs when a stable spiral changes into an unstable spiral surrounded by nearly elliptical limit cycle (Strogatz, 1994). A subcritical Hopf bifurcation occurs when small perturbation can lead to either decaying oscillations due to a stable equilibrium or a jump to a large sustained oscillations in the system due to an unstable limit cycle. For the analysis of the bifurcation type, the main challenge is the numerical stiffness, due to the nonlinear logarithmic term. The set of parameters Π does not cross the Hopf bifurcation if $\gamma > \gamma_{HB}$. Small disturbances decay after ringing for a while and stable spiral is observed. The block and the driver plate are moving at constant rate $v = 1$, and the relative position is η . On the other hand for $\gamma < \gamma_{HB}$, the parameter values cross the Hopf bifurcation. The equilibrium state loses stability and unstable spiral is observed. This type of bifurcation is expected for smooth, non-catastrophic changes. The slow earthquakes are almost imperceptible because the displacement rate is very low compared to ordinary earthquakes and they are generated for parameter values around the critical value of nucleation. Hopf bifurcation is supercritical within the proposed limits for unforced system. To find chaotic behavior or strange attractors with the non-forced system it is necessary to vary epsilon very far (Erickson *et al.*, 2008) from the value of the Hopf bifurcation that we are analyzing. However, Kostić *et al.* (2013) have found chaotic behavior for small values of Π by introducing time delay in the friction term. They have found two types of Hopf bifurcation depending on the variation of the time delay. Similarly, by introducing the external force $\tau(t)$ a subcritical Hopf Bifurcation could be given for some critical $\tau(t)$ and slight variation of the ε and ξ parameters. Disturbances do not allow the system to remain at an equilibrium point resulting in continuous oscillations or chaos. For the case when the set of parameters Π crosses the Hopf bifurcation, continuous oscillations were found in both displacement and velocity only by varying the bifurcation parameter. Determining critical values of Π and $\tau(t)$ requires more concrete study.

4 Discussion and Conclusions

We have analyzed the DR-S model which describes the kinetic mechanism during an earthquake. The system displays richness in their oscillatory dynamic behavior: from attracting cycles of one and two periods to a limit cycle and multi-periodic orbits, depending on the parameters values in the necessary condition for stability (13). The necessary condition is maintained even for a set of parameters within the frictionally unstable region. This behavior was studied by bifurcation diagrams through the Hopf bifurcation mechanism.

The complex oscillatory behavior discussed in this paper is determined by the variation of parameter γ , fixed values ε and ξ , and the necessary condition for stability (13). The necessary condition depends on the parameter γ , and this depends on the characteristic length L , suggesting that the complex oscillatory behavior should be observed for a range of values for the parameter γ . The unperturbed and perturbed cases have shown how the system describes behavior as it is found in systems

with *SSO*, this is in the case when the necessary condition (13) is maintained (Figures 7 and 9). There are self-oscillations that create multi-periodic orbits, but eventually converge to a limit cycle and the range of $u_{lmax}(t)$ decreases when γ increases.

The γ parameter seems to be relevant, and consequently the characteristic length L . Lapusta *et al.* (2000), Lapusta and Rice (2003), and Abe and Kato (2013) derived some conclusions concerned to L from laboratory experiments and numerical simulations. They associated L with the size of small earthquakes, with frequency, and *SSO*. If L decreases then the block is frictionally less stable, *i. e.*, there are more frequent displacements, moreover, they found under a range of parameters values the oscillations can change from periodic to aperiodic and conversely, but the border of the transition was not defined.

Under the assumption $B > A > 0 \Rightarrow \varepsilon > 0$ and Eq. (20), Hopf bifurcation occurs for any $\gamma \geq 0.5$ within the standard $0.4 < \xi_0 < 1$, moreover, $\varepsilon_{HB} \rightarrow \xi_0$ when γ increases in such way that for any $\gamma \geq 10$ the values of ε_{HB} are equal. For these values ε is bounded in $0 < \varepsilon_{HB} < 1$. This would have some implications related to the slow earthquakes nucleation. For *SSO* region, approximately for $0.5 < \gamma \leq 10$ the oscillation frequency and fluid are determinant for the system have unstable oscillations. For small values of γ there are more transitions in the dynamical oscillatory behavior, when the necessary condition (13) holds and does not it as it is shown in Figures 7, 9, and 10. On the other hand, for $\gamma \geq 10$ there are less transitions, neither the fluid and frictional coefficients of Stribeck in the medium affect to the oscillatory behavior ($\phi/\gamma^2 \rightarrow 0 \Rightarrow \psi \rightarrow 1$). This general behavior for small γ seems to be independent on the angular frequency, ω , of the external force because even the unperturbed system displays this behavior. The function of the ω variation is the generation of the dominant type of orbits (one, two, or more periods) and its frequency of transition which is bigger when the necessary condition fails. The complex oscillatory behavior is dependent of small γ values, and of the necessary condition for stability (13) that involves fluids from Stribeck's effect.

The relevance of γ seems to be associated with the presence of fluid. Erickson *et al.* (2008) determined that the stationary solution $x^* = (0, 0, 1)$ is independent of seismic parameters, the relative position of the block and the plate will not depend on the frictional coefficients or seismic parameters; the system would be under the limit of the stable/unstable regime where the big earthquakes are nucleated. At this solution the block and the plate have the same velocity and there is no contact with asperities, hence there is no displacement between the plate and the slider block.

Complementarily, we found if Stribeck's effect is added to the Madariaga's Model then the stationary solution $x^* = (0, \eta, 1)$ has the displacement or relative position as a function of seismic parameter γ . The parameter γ is associated with the oscillation frequency of the block as well as the frictional constants related to fluid through ψ in the necessary condition (13). The relative position u is not necessarily zero although the relative displacement is. The role of frequency oscillations and fluid is decisive for dissipation and consequently it is also for the block position. If γ is large enough then $x^* \rightarrow (0, 0, 1)$, *i. e.*, if γ or kL increases, then $u^* \rightarrow 0$. The last statement could be interpreted as k increases making the system stiffer or L increases making slower the stress drop under some conditions.

The stability analysis of x^* was through eigenvalues of Eq. (8). If the real part is negative for all eigenvalues then the stationary solution is a sink and the system is in the stable regime, the medium properties break any nucleation or propagation of earthquakes. Scholz (1998) determined a critical value for frictional stability/instability under elastic medium, with an

oscillator coupled to Dieterich friction law:

$$\bar{\sigma}_c = \frac{-kL}{a-b} \quad (24)$$

that depends on the rocks properties, point nucleation and frictional parameters $a-b$, k , y L . The critical value $\bar{\sigma}_c$ corresponds to the normal effective stress. When any $\bar{\sigma}$ holds $\bar{\sigma} \geq \bar{\sigma}_c$, then there are changes in the frictional properties, such changes unchained earthquakes. This phenomena is named frictional instability. Scholz (1998) reported that the *SSO* are into the stable regime, below the critical value of nucleation (24) (Fig. 1), on complementary way this investigation reveals that the critical value (24) of Scholz (1998) have got to the upper limit of *SSO* in the unstable region, and it is related to the upper limit of *SSO* in the frictionally unstable region regardless Stribeck's effect.

The relation between the *SSO* (23) and (24) comes from the definition of $\Pi = (\varepsilon, \xi, \gamma)$ and the statement $(A-B) = \sigma(a-b)$ (Daub and Carlson, 2008) as follows. From Eq. (24) $\bar{\sigma}_c(b-a) = kL \Rightarrow (B-A) = kL \Rightarrow (B-A)/A = kL/A \Rightarrow \varepsilon = \xi$, on the other hand $\varepsilon = \xi\psi \Rightarrow \bar{\sigma}_c(b-a)/A < kL\psi/A \Rightarrow \bar{\sigma}_c = -kL\psi/(a-b)$, a corrected value for *SSO* is as follows

$$1 < \bar{\sigma}_c^* \equiv \frac{-kL\psi}{(a-b)} \equiv \bar{\sigma}_c\psi, \quad (25)$$

which combines frictional parameters of Dieterich-Ruina friction law and Stribeck's effect. Equations (13) and (25) are equivalent. If $\gamma > 10$, $\psi \rightarrow 1$ and $\bar{\sigma}_c^* \rightarrow \bar{\sigma}_c$.

The upper limit of *SSO* behavior is a function of seismic parameters and frictional coefficients concerned to fluids although this was established for the base of seismogenic layer, it is likely probably it could be applied to the shallow transition zone in addition with the parameters and constants related to the slip-hardening (Ikari *et al.*, 2013). The fluid presence involves the frequency of oscillation of the block as a very important element to dissipation and consequently with the stationary solution (equilibrium point of the system) as well as in the upper limit proposed for slow earthquakes zone. The characteristic length L has a primary relevance on the results of this research.

20

Although this investigation is more related to the proposal of a formal pattern in the study of SSEs, and with a first approximation of the upper limit of the transition zone, this is considered as a preliminary study in order to be applied to the real seismogenic regions. However, the parameters considered for slow earthquakes are still being studied through observations, experiments, and by means of simulations, but there is still not something precise.

25 The study of SSEs in Cascadia (Watkins *et al.*, 2015) indicates a possible link between the observational and experimental data with the parameters involved in the most of models of earthquake's physic coupled to the Dieterich-Ruina's friction law. The slip amount of SSEs is in cm order but the average slip amount of smaller events are unknown. The effective normal stress in the range of 3-9 MPa produce fault slip consistent with some observed SSEs, $B-A$ is in the range (0.0015 to 0.003) of the slow slip section. At the top of the slow slip section $B-A$ is 0.003 and 0.001 at the base, $A \approx 0.02$, L is in the range 1-50 μm (real L is unknown), the rate of convergence (10 a 50 mm/year) represents the range of convergence rates of subduction zones where SSEs are observed with GPS. These parameters could vary depending on the region that SEEs occur. Further, the

30

critical value $K_c = (A - B)\sigma/L$ depend on L ; viscosity=0.1 (nondimensional) has been used in earthquake models (Carlson *et al.*, 1994), but the estimation of the real viscosity depends on the region.

The proposed upper limit for the SSEs zone includes the fluids and oscillation frequency (and consequently L), through ψ . They might be introduced into the simulations and experiments in order to see which are the implications over the recurrence times, duration and velocity of SSEs in real seismogenic regions. A final step would be using scaling laws for SSEs to determine the real values of parameters included either experimental and/or simulation data, such as the stiffness K_c and viscosity, take into account the specific characteristics of the fault.

Competing interests. The authors declare that they have no conflict of interests.

Acknowledgements. This study was supported by CONACyT (support 44731), the Departments of Applied Mathematics and Applied Geosciences of Instituto Potosino de Investigación Científica y Tecnológica (IPICYT), and the Instituto de Geología, Universidad Autónoma de San Luis Potosí, México. E. Campos Cantón acknowledges the CONACyT financial support for sabbatical at Department of Mathematics, University of Houston. He would also like to thank the University of Houston for his sabbatical support and to Professor Matthew Nicol for allowing him to work together closely and his valuable discussions on dynamical systems. The authors also acknowledge technical support from Irwin A. Díaz-Díaz.

References

- Abe, Y., and Kato, N.: Complex Earthquake Cycle Simulations Using a Two-Degree-of-Freedom Spring-Block Model with a Rate-and State-Friction Law, *Pure and Applied Geophysics*, 170(5), 745-765, 2013.
- Abe, Y. and Kato, N.: Intermittency of earthquake cycles in a model of a three-degree-of-freedom spring-block system, *Nonlinear Processes in Geophysics*, 21, 841-853, 2014.
- 5 Alvarez-Ramírez, J., Garrido, R., and Femat, R.: Control of systems with friction, *Physical Review E*, 51(6), 6235, 1995.
- Amendola, A., and Dragoni, M.: Dynamics of a two-fault system with viscoelastic coupling, *Nonlinear Processes Geophysics*, 20, 1-10, 2013.
- Andersson, S., Söderberg, A., and Björklund, S.: Friction models for sliding dry, boundary and mixed lubricated contacts, *Tribology international*, 40(4), 580-587, 2007.
- 10 Audet, P., and Bürgmann, R.: Dominant role of tectonic inheritance in supercontinent cycles, *Nature Geoscience*, 4(3), 184-187, 2011.
- Baca, D.: Análisis paramétrico de la bifurcación de Hopf en sistemas tipo Lorentz, Tesis: Universidad de Sonora, Hermosillo, México, (2007).
- Batista, A. A., and Carlson, J. M.: Bifurcations from steady sliding to stick slip in boundary lubrication, *Physical Review E*, 57(5), 4986, 1998.
- 15 Beroza, G. C., and Ide, S.: Deep tremors and slow quakes, *Science*, 1025-1026, 2000. doi:10.1126/science.1171231
- Brown, K. M., Tryon, M. D., DeShon, H. R., Dorman, L. M., and Schwartz, S. Y.: Correlated transient fluid pulsing and seismic tremor in the Costa Rica subduction zone, *Earth and Planetary Science Letters*, 238 (12), 189-203, 2005.
- Bürgmann, R.: Earth science: Warning signs of the Iquique earthquake, *Nature*, 512(7514), 258-259, 2014.
- Campos-Cantón, E., Barajas-Ramírez, J. G., Solís-Perales, G., and Femat, R.: Multiscroll attractors by switching systems, *Chaos*, 20(1), 20 013116, 2010.
- Carlson, J. M., Langer, J. S., and Shaw, B. E.: Dynamics of earthquake faults, *Reviews of Modern Physics*, 66, 657-670, 1994.
- Carlson, J. M., and Batista, A. A.: Constitutive relation for the friction between lubricated surfaces, *Physical Review E*, 53, 4153-4165, 1996.
- Castellanos-Rodríguez, V. and Femat, R.: A model for earthquakes based on friction effects: Oscillatory aperiodic behavior, *Analysis and Control of Chaotic Systems*, 3, 115-120, 2012.
- 25 Chelidze, T., Matcharashvili, T., Gogiashvili, J., Lursmanashvili, O., and Devidze, M.: Phase synchronization of slip in laboratory slider system, *Nonlinear Processes in Geophysics*, 12, 163-170, 2005.
- Daub, E. G. and Carlson, J. M.: A constitutive model for fault gouge deformation in dynamic rupture simulations, *Journal of Geophysical Research, Solid Earth*, 113, B12, 2008, doi: 10.1029/2007JB005377.
- Davis, E., Heesemann, M., and Wang, K.: Evidence for episodic aseismic slip across the subduction seismogenic zone of Costa Rica: CORK borehole pressure observations at the subduction prism toe, *Earth and Planetary Science Letters*, 306, 299-305, 2011. doi:10.1016/j.epsl.2011.04.017
- 30 De sousa Vieira, M.: Chaos in a simple spring-block system, *Physics Letters A*, 198 (5-6), 407-414, 1995. 10)
- Dieterich, J. H.: Modeling of Rock Friction, 1, Experimental Results and Constitutive Equations, *Journal of Geophysical Research*, 84, 2161-2168, 1979.
- 35 Dieterich, J. H., and Kilgore, B. D.: Direct observation of frictional contacts: New insights for state-dependent properties, *Pure and Applied Geophysics*, 143(1-3), 283-302, 1994.

- Di Toro, G., Han, R., Hirose, T., De Paola, N., Nielsen, S., Mizoguchi, K., Ferri, F., Cocco, M., and Shimamoto, T.: Fault lubrication during earthquakes, *Nature*, 471, 494-498, 2011.
- Dragert, H., Wang, K., and James, T. S.: A Silent Slip Event on the Deeper Cascadia Subduction Interface, *Science*, 292 (5521), 1525-1528, 2001.
- Dragoni, M., and Piombo, A.: Dynamics of seismogenic fault subject to variable strain rate, *Nonlinear Processes in Geophysics*, 18, 431-439, 5 2011.
- Dragoni, M., and Santini, S.: Simulation of the long-term behaviour of a fault with two asperities, *Nonlinear Processes in Geophysics*, 17, 777-784, 2010.
- Erickson, B., Birmir, B., and Lavallée, D.: A model for aperiodicity in earthquakes, *Nonlinear Processes Geophysics*, 15, 1-12, 2008.
- Faulkner, D. R., Jackson, C. A. L., Lunn, R. J., Schlische, R. W., Shipton, Z. K., Wibberley, C. A. J., and Withjack, M. O.: A review of 10 recent developments concerning the structure, mechanics and fluid flow properties of fault zones, *Journal of Structural Geology*, 32 (11), 1557-1575, 2010.
- Gee, M. L., McGuiggan, P. M., Israelachvili, J. N., and Homola, A. M.: Liquid to solidlike transitions of molecularly thin films under shear, *Journal of Chemical Physics*, 93, 1895, 1990.
- Gu, J., Rice, J. R., Ruina, A., and Tse, S.: Slip motion and stability of a single degree of freedom elastic system with rate and state dependent 15 friction, *Journal of the Mechanics and Physics of Solids*, 32, 167-196, 1984.
- Guckenheimer, J., and Holmes, P.: *Nonlinear oscillations, dynamical systems, and bifurcations of vector fields*, (Vol. 42). Springer Verlag: New York, 1983.
- Ide, S., Beroza, G. C., Shelly, D. R., and Uchide, T.: A scaling law for slow earthquakes, *Nature*, 447, 76-79, 2007. doi: 10.1038/nature05780.
- Ikari, M. J., Marone, C., Saffer, D. M., and Kopf, A. J.: Slip weakening as a mechanism for slow earthquakes, *Nature Geoscience*, 6, 468-472, 20 2013.
- Jacobson, B.: The Stribeck memorial lecture, *Tribology International*, 36, 781-789, 2003.
- Jolivet, R., Lasserre, C., Doin, M., Peltzer, G., Avouac, J., Sun, J., and Dailu, R.: Spatio-temporal evolution of aseismic slip along the Haiyuan fault, China: Implications for fault frictional properties. *Earth and Planetary Science Letters*. 377-378, 23-33, 2013, doi:10.1016/j.epsl.2013.07.020
- 25 Kengne, J., Kenmogne, F., and Kamdoum Tamba, V.: Experiment on Bifurcation and Chaos in Coupled Anisochronous Self-Excited Systems: Case of Two Coupled van der Pol-Duffing Oscillators, *Journal of Nonlinear Dynamics*, vol. 2014, Article ID 815783, 13 pages, 2014.
- Khalil, M.: *Nonlinear Systems*, Second edition. Prentice-Hall, 1996.
- Kostić, S., Franović, I., and Todorović, K.: Friction memory effect in complex dynamics of earthquake model, *Nonlinear Dynamics*, 73, 1933-1943, 2013. doi:10.1007/s11071-013-0914-8.
- 30 Lapusta, N. and Rice, J.: Nucleation and seismic early propagation of small and large events in a crustal earthquakes model, *Journal of Geophysical Research*, 108, 765 (2003).
- Lapusta, N. and Rice, J., Ben-Zion, Y., and Zheng, J.: Elastodynamic analysis for slow tectonic loading with spontaneous rupture episodes on faults with rate-and state-dependent friction, *Journal of Geophysical Research*, 105, 765 (2000).
- Levin, V. W.: Non-linear oscillating structures in the earthquake and seaquake dynamics, *Chaos*, 6(3), 405-413, 1996.
- 35 Maloney, C. E., and Robbins, M. O.: Shear faults in a model brittle solid, *Chaos*, 17, 041105, 2007.
- Marone, C., Scuderi, M., Leeman, J., Saffer, D., Collettini, C., and Johnson, P.: Slow earthquakes and the mechanics of slow frictional stick-slip, *Geophysical Research Abstracts*, Vol. 17, EGU2015-9533, EGU General Assembly 2015.

- Nishimura, T.: Short-term slow slip events along the Ryukyu Trench, southwestern Japan, observed by continuous GNSS. *Prog. Earth and Planetary Science*, 1, 22 (2014).
- Peng, Z., and Gomberg, J.: An integrated perspective of the continuum between earthquakes and slow-slip phenomena, *Nature Geoscience*, 3(9), 599-607, 2010.
- Perko, M.J., Jarnvig, I. L., Hojgaard-Rasmussen, N., Eliassen, K., and Arendrup, H.: Electric impedance for evaluation of body fluid balance
5 in cardiac surgical patients, *Journal of cardiothoracic and vascular anesthesia*, 15(1), 44-48, 2001.
- Reiter, G., Demirel, A. M., and Granick, S.: From Static to Kinetic Friction in Confined Liquid Films, *Science*, 263 (5154), 1741-1744, 1994.
- Rivet, D., Campillo, M., Shapiro, N. M., Cruz-Atienza, V., Radiguet, M., Cotte, N., and Kostoglodov, V.: Seismic evidence of nonlinear crustal deformation during a large slow slip event in Mexico, *Geophysical Research Letters*, 38, 2011. L08308, doi:10.1029/2011GL047151.
- Ruina, A.: Slip instability and state variable friction laws, *Journal of Geophysical Research: Solid Earth*, (1978-2012), 10359-10370, 1983.
- 10 Saffer, D., and Wallace, L. M.: The frictional, hydrologic, metamorphic and thermal habitat of shallow slow earthquakes. *Nat. Geosci.* 8, 594-600, 2015. doi: 10.1038/ngeo2490
- Scholz, C. H.: Earthquakes and friction laws, *Nature*, 391.6662, 37-42, 1998.
- Scuderi, M., Marone, C., Tinti, E., Scognamiglio, L., Leeman, J., Saffer, D., Di Stefano, G., and Collettini, C.: Seismic velocity changes across the transition from slow-to fast-frictional sliding in earthquake-like laboratory experiments. AGU Chapman Conference in the
15 Slow Slip Phenomena, Ixtapa, Guerrero, Mexico, 21-26 february 2016.
- Shkoller, S. and Minster, J. B.: Reduction of dieterich-ruina attractors to unimodal maps, *Nonlin. Processes Geophys.*, 4, 63-69, 1997.
- Strogatz, S.H: *Nonlinear Dynamics and Chaos: with application to physics, biology, chemistry, and engineering*, (Perseus Book Publishing, 1994).
- Thomas, A., Beroza, G., and Shelly, D.: Constraints on the source parameters of low-frequency earthquakes on the San Andreas Fault.
20 *Geophysical Research Letters*, 43, 1464-1471, 2016. doi: 10.1002/2015GL067173
- Valée, M.; Nocquet, J., Battaglia, J., Font, Y., Segovia, M., Régnier, M., Mothes, P., Jarrin, P., Cisneros, D., Vaca, S., Yepes, H., Martin, X., Béthoux, N., and Chlieh, N.: Intense interface seismicity triggered by a shallow slow slip event in the Central Ecuador subduction zone, *Journal of Geophysical Research*, 118, 2965-2981, 2013.
- Vergnolle, M., Walpersdorf, A., Kostoglodov, V., Tregoning, P., Santiago, J. A., Cotte, N., and Franco, S. I.: Slow slip events in Mexico
25 revised from the processing of 11 year GPS observations, *Journal of Geophysical Research*, 115, 2010. doi: 10.1029/2009JB006852
- Wang, H., Yu, Y., and GuoguangWen: Dynamical Analysis of the Lorenz-84 Atmospheric Circulation Model, *Journal of Applied Mathematics*, vol. 2014, Article ID 296279, 15 pages, 2014.
- Watkins, W. D., Colella, H. V., Brudzinski, M. R., Richards-Dinger, K. B., and Dieterich, J. H.: The role of effective normal stress, frictional properties, and convergence rates in characteristics of simulated slow slip events, *Geophysical Research Letters*, 42,
30 doi:10.1002/2014GL062794.
- Wallace, L. M., Webb, S. C., Ito, Y., Mochizuki, K., Hino, R., Henrys, S., Schwartz, S., and Sheehan, A.: Slow slip near the trench at the Hikurangi subduction zone, New Zealand, *Science*, 352, 701-704, 2016, doi: 10.1126/science.aaf2349
- Wech, A. G., and Creager, K. C.: Cascadia tremor polarization evidence for plate interface slip, *Geophysical Research Letters*, 34(22), 2007.
- Xin-YouMeng and Hai-Feng Huo: Bifurcation Analysis of a Lotka-Volterra Mutualistic System with Multiple Delays, *Abstract and Applied*
35 *Analysis*, vol. 2014, Article ID 958140, 18 pages, 2014.

Yamashita, Y., Yakiwara, H., Asano, Y., Shimizu, H., Uchida, K., Hirano, S., Umakoshi, K., Miyamachi, H., Nakamoto, M., Fukui, M., Kamizono, M., Kanehara, H., Yamada, H., Shinohara, M., and Obara, K.: Migrating tremor off southern Kyushu as evidence for slow slip of a shallow subduction interface, *Science*, 348, 676-679, 2015. doi: 10.1126/science.aaa4242 pmid:25954006

Yoshizawa, H., and Israelachvili, J.: Fundamental mechanisms of interfacial friction. 2. Stick-slip friction of spherical and chain molecules, *Journal of Physical Chemistry*, 97 (43), 11300-11313, 1993.

- 5 Zhang, Y. and Martin Golubitsky, M.: Periodically Forced Hopf Bifurcation, *SIAM Journal of Applied Dynamical Systems*, 10(4), 1272-1306, 2011.